A Reconfigurable Multiband Antenna for RFID and GPS Applications

Norsuzlin Mohd Sahar[1], Muhammad Tariqul Islam[1], Norbahiah Misran[1]
[1]*Department of Electrical Electronic & Systems Engineering, The National University of Malaysia, 43600 UKM Bangi, Selangor, Malaysia*
norsuzlin@siswa.ukm.edu.my

***Abstract*—A C-shaped patches loaded with dipole antenna designed for multiband antenna is proposed. The antenna can be reconfigured as single band at 1.2275 GHz for GPS applications and dual-band frequencies at UHF band (850 MHz–930 MHz) and ISM band (2.41 GHz–2.54 GHz) required in RFID applications. The performance of the antenna involves changing the switches to ON or OFF mode by controlling switches. By adjusting the dimension of C-shaped patch, a dual-band frequency of 0.89 GHz and 2.46 GHz is performed. The antenna's gains are 2 dBi and 3.2 dBi for lower and upper bands respectively. The length slot and length of C-shaped patch can be varied to adjust the desired upper frequency as well as the bandwidth. Moreover, the lower frequency can be tuned by varying the dipole arms for both elements. Nevertheless, the dipole antenna operated as single band when the switches are OFF at frequency resonance is 1.2275 GHz with 2.06 dBi of gain. The total efficiency for single and dual band is greater than 90 %. The design methodology and antenna measurement results are both presented and discussed in this paper.**

***Index Terms*—Reconfigurable antenna, dipole, RFID, GPS, ominidirectional.**

I. INTRODUCTION

A reconfigurable multiband antenna has led to great demand component for the mobile devices that can operate several frequency bands for different communication systems and standards. By selecting different antenna switch mode, several of communication systems include GSM, DCS, PCS, UMT, Bluetooth and WLAN can be served by one antenna. Several approaches have been proposed in the implementation of the frequency reconfigurable antenna. Most of these approaches use either electronic or electromechanical switches [1]–[3] where the ON or OFF mode are controlled. In [1], an RF MEMS switch was applied to change the slot dimensions in improving the impedance bandwidth for the E-patch antenna. RF MEMs has been chosen due to the satisfactory RF properties includes low insertion loss, good impedance matching and high isolation. PIN diodes were demonstrated in [2] to achieve dual band polarization reconfigurable antenna. The antenna can radiate horizontal, vertical or 45° linear polarization by switching the PIN diodes. Different types of switches have different advantages to be applied in certain design. The switch was proposed in [3] for the reconfigurable multiband antenna to switch ON and OFF two patches antenna two operates antenna in two different dual band mode or wideband mode.

Reconfigurable multiband antenna demonstrated in some papers can be switched from single narrowband to another single narrowband [4], between dual band to another dual band [5] and multiband to other multiband configurations [6]. Proposed antenna in [4] by having 5 PIN diodes switches to serve switchable multiband operations of the antenna that can operate, one at a time at five adjacent frequencies sub bands in UWB. Differently in [6], the antenna that can switch to single, dual or triple band modes was proposed. The slot was designed to control the arms of the dipole either switch in and out from the slot edges.

Several methods were approached in design the multi-frequency from a single antenna. In [7], the dual band functionality was achieved though a perturbation method by coupling an electrically a two-turn spiral resonator to the antenna. The position of the resonators along the line affects the characteristic impedance. Dual operating frequencies also were achieved by loading two pairs of narrow slots in the triangular patch [8]. By adjusting the slot, protruding a narrow slot out of embedded slots close to the side edges; broad-band radiation was obtained. A triple band also was proposed by employed a cross slot in the ground plane in [9]. Other methods were by integrated with the dipoles printed on the same substrate to perform triple band with directional radiation pattern [10]. It consist a top loaded dipole for lower frequency, two longer dipoles for middle frequency and two shorter dipoles for upper frequency. Thus, the integration by two patches is implemented in this paper to achieve two frequency bands.

With the rapid development of Radio Frequency Identification technology in service industries and commercial wireless applications, many papers were presented in the literature [11]–[17]. Most of RFID antennas were designed to operate at one or more frequency bands, Low Frequency, High Frequency, Ultra High Frequency, and Microwave. Each of frequency bands has their own advantages. Thus, the urge of multiband RFID antennas is becoming vivid. As a result, there are many papers were designed a multiband antenna for RFID applications which was applicable for several standards [11]. Due to different worldwide regulations, the frequency bands have different locations in the spectrum. For an example is UHF-RFID

Manuscript received June 5, 2015; accepted October 12, 2015

application, Europe operates at 855 MHz–869 MHz, US at 902 MHz–928 MHz and Japan 950 MHz–928 MHz [12] Moreover ISM-RFID operates at 2.45 GHz and 5.8 GHz. In [13], a dual band passive RFID tag antenna applicable for recessed cavity in metallic objects by artificial magnetic conductor – AMC plane to provide UHF bands for European band (869.5 MHz–869.7 MHz) and Korean bands (910 MHz–914 MHz) was proposed. With the same UHF RFID bands, S-shaped RFID tag antenna mountable on metallic surface with a meander and spiral structure in compact size and narrow band was designed [14].

Recently, UHF and ISM bands become popular to be designed as dual band antennas for RFID long range application [15]–[17]. In [15], a dual band frequency was performed by controlling the shape and size of the diamond shape patch. The bandwidth was 18 MHz (902 MHz–920 MHz) in UHF band and 80 MHz (2.42 GHz–2.5 GHz) in ISM band with the size of the antenna was 150 mm × 127 mm × 5 mm. The antenna bandwidth was expanded by utilizing the coupling effect between the notched patch and the resonant aperture for dual-band RFID reader antenna 155 mm × 230 mm in size [16]. In developing an advance tracking system, RFID and GPS antenna are important_technologies as tracking and locator system. In order to achieve that, the new integration design for UHF RFID and GPS was presented in [18].Two types of substrate were needed, TLX-9 substrate and FR-4 substrate and by optimizing printed quadrifilar antennas (PQAs) to operate two different resonant frequencies. The compactness of integration is required to mountable on any product as portable device. Thus, the reconfigurable antenna is one of the most suitable antennas for operate both system, RFID and GPS.

In this paper, a simple structure antenna operating as single band for GPS application and dual band, UHF and ISM bands for RFID applications is proposed. The proposed antenna uses a single substrate and no ground plane is required. The C-shaped patches perform as a radiating element is loaded with a basic dipole antenna to achieve a dual band antenna is presented. The optimized antenna is prototyped and tested for verification. The methodology as well as discussions on both simulation and measurement is presented in the subsequent sections

II. ANTENNA DESIGN

A. Dipole Antenna Design

The proposed antenna is designed on a Fire Retardant-4 board (FR4) with the dimension of 90 × 25 mm^2 in size which has a relative dielectric constant of ε_r = 4.7 with tangent loss of 0.019 and it has a 1.6 mm substrate thickness and a 0.035 mm copper thickness. A planar dipole antenna is designed as the basic antenna resonating as lower band with omni-directional radiation pattern. The structure of the dipole antenna consist of two dipole arms which are located at the same sides of the board as depicted in Fig. 1. *L1* is the length of the arm dipole and *W1* is the width of the arm dipole. It is symmetrical of dipole arms with the gap between the dipole length is 1 mm. The L2 × W2 connects to the port (SMA connector) to one of two dipole arms underneath of the board. Another dipole arm is connected as a ground. For this proposed antenna, ground plane are not required. The final dimensions of the optimized dipole loaded with C-shaped patch structure is shown on Table I. The optimization is done by two parts. For a single band, theory of dipole antenna is applied by varying the parameters of L1, W1, L2 and W2. For the dual band frequencies, the C-shaped patch structure is analysed for the parameters *a*, *b*, *c* and *d* as explained in part c. The slot dimension (*a* mm × *b* mm) is caused the frequency of resonant and bandwidth for upper band. The analysis is done within the range of 5 mm ≤ *a* ≤ 13 mm and 13mm ≤ *b* ≤ 19 mm. The lower band is performed depends on the length of dipole and the size of rectangular patch (*c* mm × *d* mm). The range of length, c is analysed from 19 mm to 27 mm and for the length of d, from 18 mm to 22 mm.

TABLE I. OPTIMIZED PARAMETERS OF THE PROPOSED ANTENNA.

Parameter	Value (mm)
L1	38.5
W1	4
L2	3
W2	15
a	9
b	19
c	19
d	22

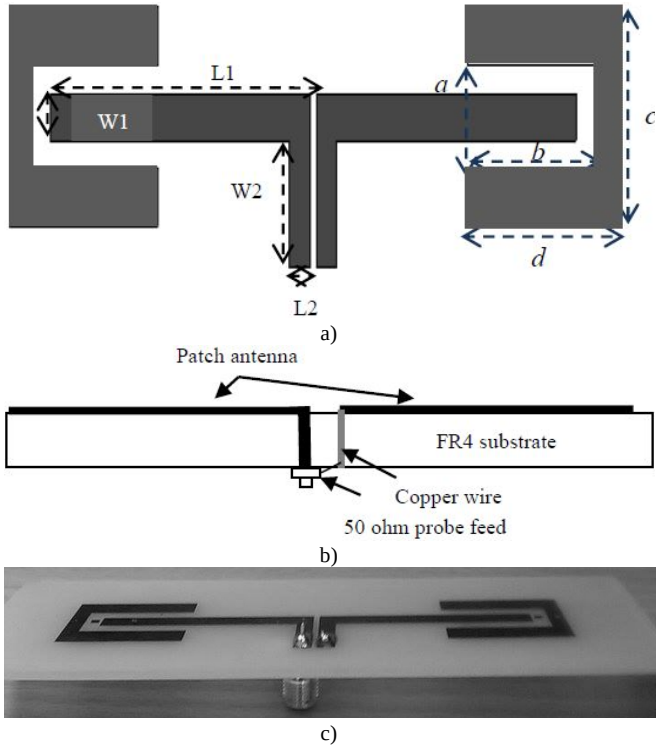

Fig. 1. Geometry of basic dipole and C-shaped patch (a); the structure of FR4 substrate (b); prototype of proposed antenna (c).

In design process, the single band is performed when the dipole antenna is radiated. The operating frequency can be tuned by adjusting the electrical length of the antenna. Thus, L_1, the length of both arms element are adjusted equally at both side and the width of dipole *W1* is constant to vary the frequency response. The dipole is designed less than half a wavelength long as required to get better performance. A

good approximation is 0.47 times the wavelength [19]. Therefore the length is calculated as shown below

$$L_1 = 0.47\frac{v}{f}, \quad (1)$$

where v is the actual propagation speed on the dipole radials and f is the resonant frequency. This speed depends on the effective dielectric constant of the environment surrounding the arms. The speed is calculated with the equation

$$v = \frac{c}{\sqrt{\varepsilon_{eff}}}, \quad (2)$$

where c is the speed of light in vacuum and ε_{eff} is the effective dielectric constant of the surrounding media. The effective dielectric constant for a printed arm on a substrate depends on the geometry and the dielectric constant of the substrate.

B. C-shaped Patch Concept

Basic dipole and C-shaped patch antennas configuration are discussed based on the current distribution as shown in Fig. 2 by using CST software. The arrow is highlighted with the black colour to study how the current distribution along the path for different dimensions. In Fig. 2(a), dipole performs a single resonant as the current distributions resonate along the dipole length, L1. A single resonant is still achieved when the dipole loaded with a rectangular patch as depicted in Fig. 2(b). As the result, the operated frequency is decreased as the current flows over a longer geometrical path.

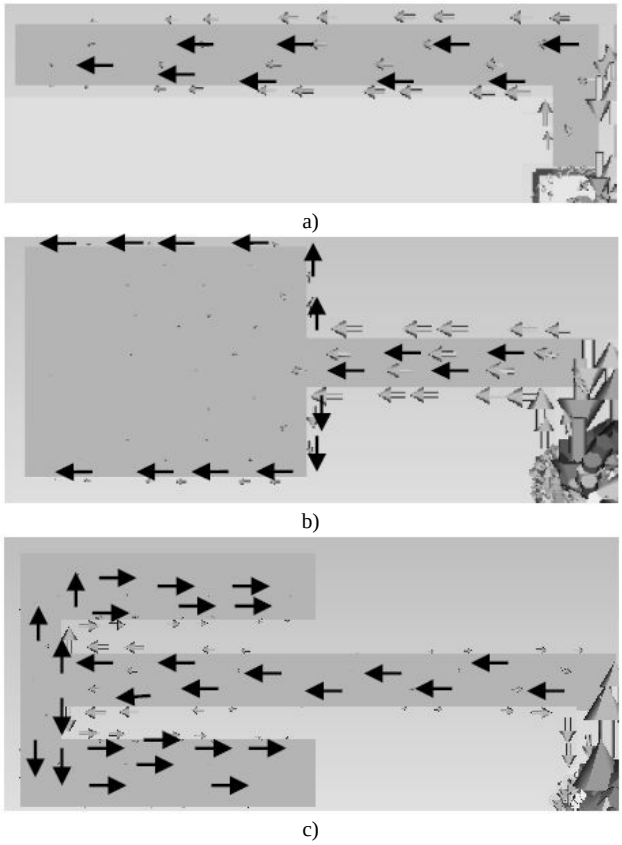

a)

b)

c)

Fig. 2. Current distribution of one side element: (a) single length of dipole; (b) single length of dipole loaded with rectangular patch; (c) single element of dipole loaded with C-shaped patch.

By introducing the slots in the rectangular patch, the distribution of the current is similar to the E-shaped patch current flows as shown in Fig. 2(c).The slot dimension of patch can be adjusted to provide a desired impedance matching performance [1]. Thus, the concept of E-shaped patch antenna is applied. Typically, the E-shaped patch antenna was presented in literature for dual resonance [1], [20] and wideband [21], [22] due to the slot dimensions that was introduced in patch.

C. Effects of Varying Parameters of C-shaped Patch

The proposed rectangular patch ($c \times d$) as a radiating element is designed to be loaded with dipole antenna in supporting strong currents and radiation at resonance. As shown in Fig. 1, structure of C-shaped patch is described where a is slot width, b is the slot length, c is the length of the rectangular patch and d is the length of the rectangular patch. The combined structure of C-shaped patches antenna and the dipole antenna at both length elements is found to be resonating at dual band. The analysis of the return loss curves when a is varied is shown in Fig. 3. The rectangular patch 19 × 22 mm^2 is loaded with dipole antenna (when a = 0), only a single resonance frequency is performed at 1 GHz. The difference of operating frequency between single dipole and loaded dipole is 30 % caused by the length of dipole arm is increased about 15 % after loaded with the C-shaped patches. The length of loaded dipole's arm is increased about 44.5 mm [L1 + gap of the two patches + $(d - b)$]. When the length of a is increased greater than the dipole width ($a > W1$), the excited surface current has produced the upper resonant frequency as the slot is introduced. Thus, a dual band is achieved. As the result, the lower band frequency also slightly changed. Thus, as the value of a is varied in the range, 5 mm ≤ a ≤ 13 mm, the range of lower frequency is decreased from 0.951 GHz to 0.885 GHz and the range of upper frequency is increased from 2.367 GHz to 2.499 GHz.

Secondly the analysis of slot length is done by varied by the range of 13mm ≤ b ≤ 19 mm as remaining the value of a = 9 mm, c = 19 mm and d = 22 mm. By altering the dimension of value b, the bandwith for upper band are effected and the bandwith of lower band is remain constant. When the slot length is reduced, the performance of bandwidth and frequency resonant are changed. However, the bandwidth of lower frequency not much changes, almost 80 MHz when the value of b is increased by 13 mm, 15 mm, 17 mm and 19 mm. On the other hand, the resonant frequency of upper band is raised to higher frequency as the value of b is decreased. Thus, the length slot dimension is caused the frequency of resonant and bandwidh for upper band is changed.

As shown in Fig. 4, the upper frequency can be adjusted when value of d is varied between the range 18 mm ≤ d ≤ 22 mm by remaining the value of a = 9 mm, b = 19 mm and c = 19 mm to perform a required upper frequency. However, the length of dipole arms must be remained as 44.5 mm. As the value of d increasing, the lower frequency resonant is slightly decreased from 0.921 GHz to 0.885 GHz with the small differences of changes that are about 3 %. The large changes of operating frequency can be seen at upper

frequency with percentage of differences at almost 10 %, and the range is decreasing from 2.706 GHz to 2.499 GHz.

Finally, the analysis of *c* value of C-shaped patches which is caused the resonant frequency of lower band effected. The width of rectangular patch is varied between the range, 19 mm ≤ *c* ≤ 27 mm. Consequently, the lower frequency is decreased from 0.89 GHz to 0.81 GHz as the value of *c* is increased within the range. The percentage of the differences of lower frequency is almost 2.3 % when the *c* is adjusted with 19 mm, 21 mm, 23 mm, 25 mm and 27 mm. However the percentage of differences for upper frequency is small, 0.3 % where the frequency range is from 2.466 GHz to 2.493 GHz.

In operating as a reconfigurable multiband antenna, the switch is placed in between the dipole arm and the C- shaped patch antenna for both elements. These two switches are operated at the same time either switch-on or switch-off Ideal switches are designed in conneting two radiating patches for the simulation purpose using CST software. In this model assumption, the switch-off is represented by open circuit and switch-on is represented by short circuit.

D. MEMs Switches

In this design, the RMSW101, Single Pole Single Throw (SPST) RF Switch is utilizing in the proposed antenna. The switch delivers high linearity, high isolation, and low insertion loss in a chip-scale package configuration [1]. In placing the switch, the gap, 1.5 mm is designed between a dipole arm and C-shaped patch. A square 1 mm^2 in size is designed at both arm length to place the switches as shown in Fig. 5.

The MEMs switch demand a 90 VDC applied to the gate actuation. To operate the MEMs switch properly, the source and drain of the switch should maintain voltage 0 V. The direct integration of dc bias line is designed to actuate the switch and the patch antenna is connected to dc ground plane to have the dc continuity. When the switch is OFF at voltage 0 V, a dipole antenna is operated as a single band. When the switch is ON, the direct current path is created across the gap between the two patches which is resonating a lower and upper frequency.

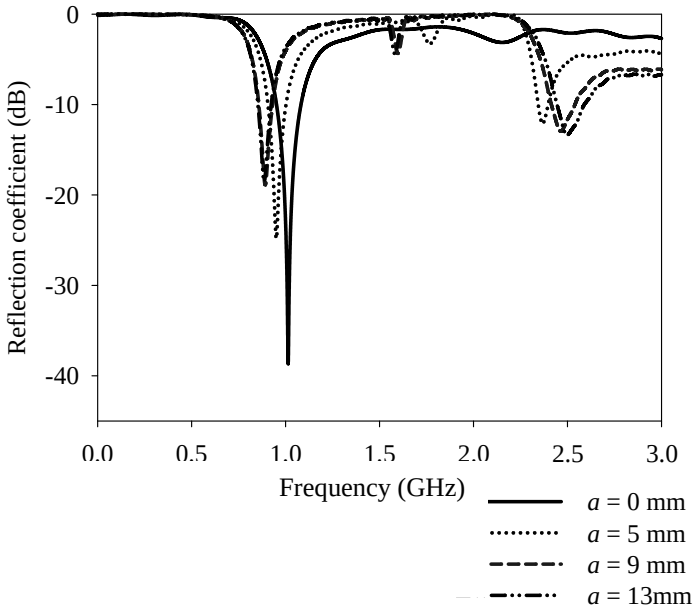

Fig. 3. Reflection coefficient versus frequency given different values of slot width *a*.

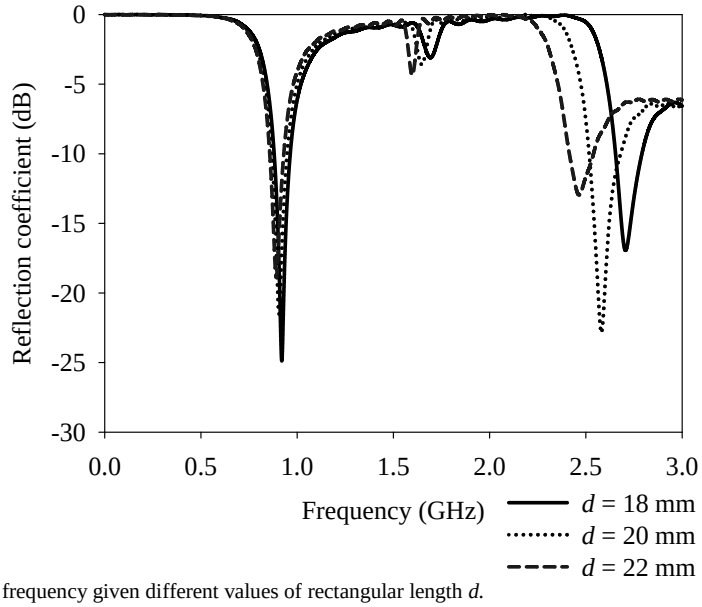

Fig. 4. Reflection coefficient versus frequency given different values of rectangular length *d*.

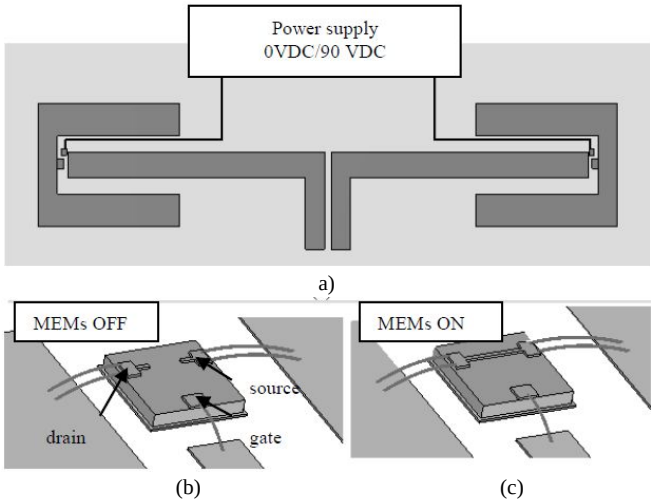

Fig. 5. Proposed antenna with two MEMs switch (a); when the MEMs switch is OFF (b); when the MEMs switch ON (c).

The wirebond are used to connect the source to the dipole arm, connect the drain to the C-shaped patch and the gate is connected to the dc supply via bias line. To isolate the actuation of the two switches, the sources and drain of both switches are the dc potential which is applied through their respective gate of the switch.

III. Result and Discussions

The design and development of the proposed antenna is achieved by using Computer Simulation Technology software (CST) where the performance of the proposed antenna can be thoroughly studied when both switches are OFF or ON state. Here, the simulated and measured reflection coefficient of the prototype is presented (Fig. 6) by using vector network analyser. A good agreement between the simulated and measured return loss of the prototype has shown. However, the differences have occurred due to effect of switches and SMA connector soldering and fabrication tolerances.

According to simulated reflection coefficient at 1.2275 GHz is -23.14 dB and the bandwidth is 140 MHz. However, the measured reflection coefficient curve the proposed antenna is excited at 1.38 GHz with a -47.23 dB performs the bandwidth greater than simulated value that is 344 MHz satisfies the (<-10 dB) when the switches are OFF state. The difference percentage is about 56 %. The simulated gain and directivity of the proposed antenna are 2.06 dBi and 2.135 dB respectively. The radiation efficiency is performed better which is 98.3 %.

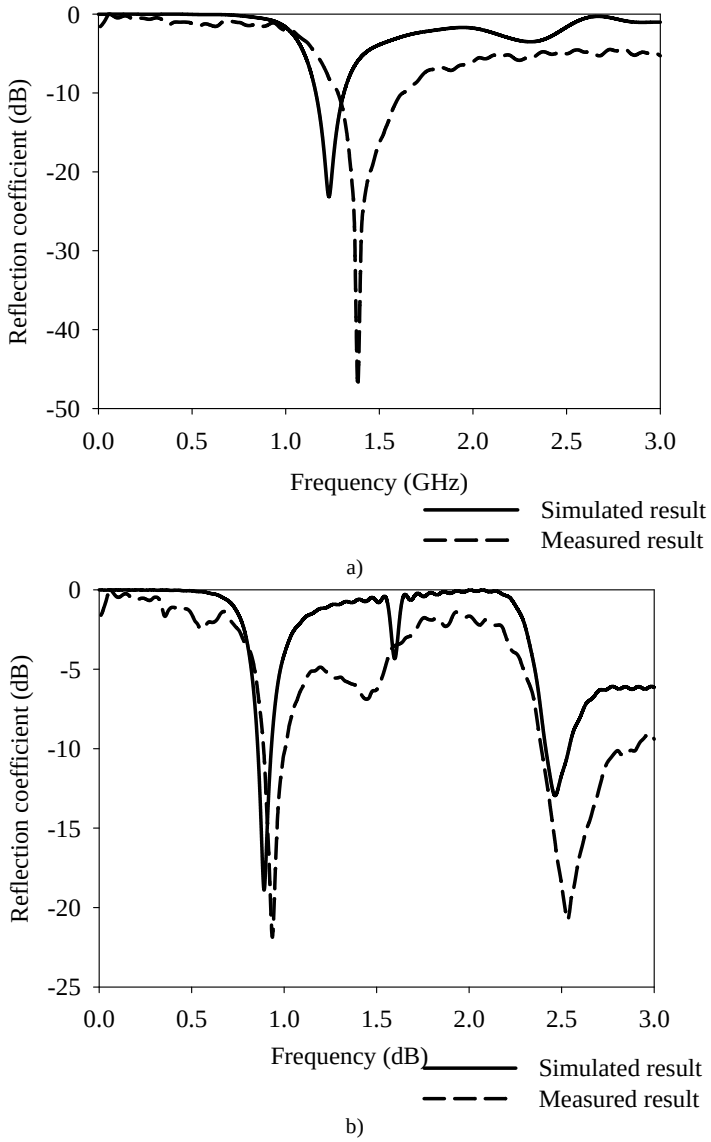

Fig. 6. Comparison simulated and measured return loss of prototype antenna: (a) when both switches are OFF, and (b) when both switches are ON.

A proposed dual-band antenna is performed when the switches are ON state. Based on the Table III, the lower band of measured reflection coefficient is excited at 0.933 GHz with –21.9 dB return loss. The percentage of differences between simulated and measured resonant frequency is 4.8 %. In addition, the measured reflection coefficient is better than simulated. For the upper band, the frequency resonance of the proposed antenna is 2.52 GHz with –20 dB return loss. The bandwidths for lower and upper bands are 113 MHz and 206 MHz respectively. As compared with the simulated bandwidth, measured dual band bandwidths are greater with the percentages are 38 % and 36.8 %. The desired frequencies are performed below –15 dB where a narrowband characteristic is shown. It is useful to minimize the potential interference. The gain of lower band is 2 dBi and the directivity is 1.97 dB. However, the gain and directivity for the upper band is greater than lower band which is 3.29 dBi and 3.31 dB respectively.

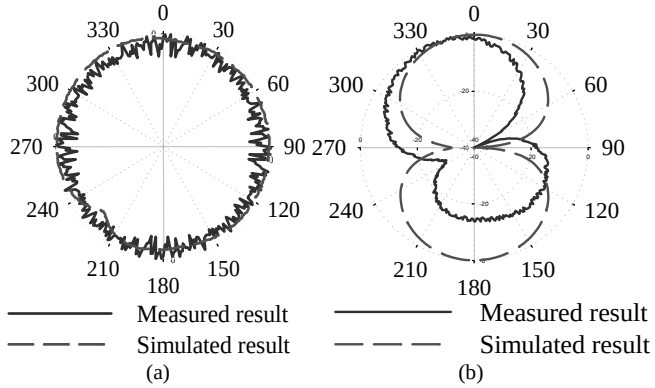

Fig. 7. Radiation patterns of prototype when both switches are OFF at 1.2275 GHz: (a) H planes, (b) E planes.

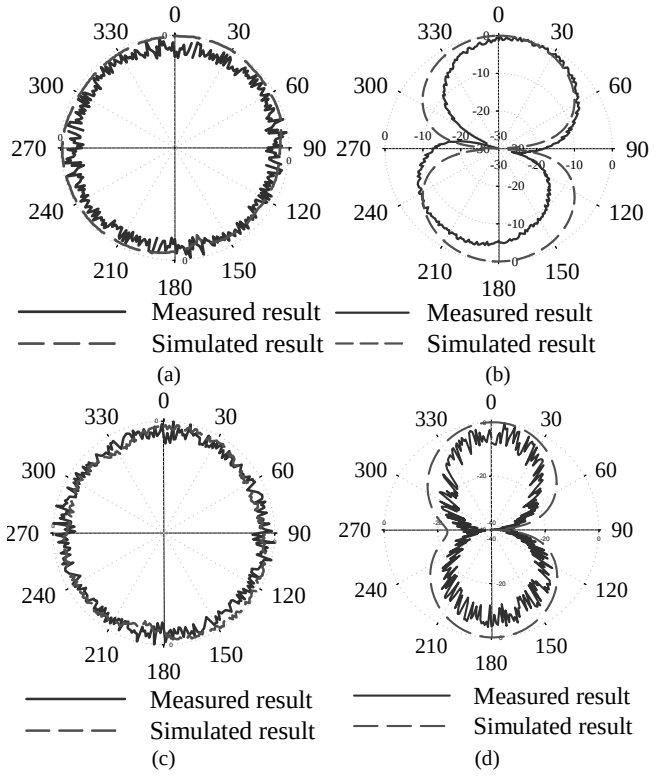

Fig. 8. Radiation patterns of prototype when both switches are ON: (a) H plane at 0.89 GHz, (b) E plane at 0.89 GHz, (c) H plane at 2.45 GHz, (d) E plane at 2.45 GHz.

TABLE II. COMPARISON RESULTS WHEN BOTH SWITCHES ARE OFF STATE.

When switches are OFF state	Simulated result	Measured Result
Frequency Resonance (Ghz)	1.2275	1.38
Reflection coefficient (dB)	-23.14	-47.23
Bandwidth (GHz)	1.16-1.30	1.28-1.62

TABLE III. COMPARISON RESULTS WHEN BOTH SWITCHES ARE ON STATE.

When switches are ON state	Simulated result		Measured Result	
	Lower band	Upper band	Lower band	Upper band
Frequency Resonance (GHz)	0.89	2.46	0.933	2.52
reflection coefficient (dB)	–18.89	–12.95	–21.903	–20.64
Bandwidth (GHz)	0.86–0.93	2.41–2.54	0.89–1.00	2.37–2.58

Secondly, the radiation patterns of E-plane and H-plane patterns are discussed to describe the performance of the antennas. The E-plane contains electric field vector and direction of maximum radiation. On the other hand, the plane that contains a magnetic field vector and direction of maximum radiation is the H-plane. The radiation patterns of different states are shown in Fig. 7 and Fig. 8. When the switch is OFF, the radiation pattern at 0.89 GHz omnidirectional radiation pattern is performed in H-plane and bidirectional in E-plane like a dipole. Besides, when the switch is ON state, the pattern is distorted a bit from the omnidirectional patterns at upper frequency at 2.45 GHz as depicted in Fig. 8(c), Fig. 8(d). This frequency corresponds to the mode where the current travel around the C-shaped patches. It is observed that the patterns resulted from the measurements have many ripples in amplitude due to many reflections into the field between the AUT and reference antenna. The reflections may come from the room floor and ceiling, chamber scattering and track inside the anechoic chamber.

IV. CONCLUSIONS

The C-shaped patch loaded with dipole antenna is being proposed. This design will be able to reconfigure the frequency band of the antenna by switches in controlling the current flow through the radiating C-shaped patches. A single dipole is operated when the switches are OFF excited at 1.2275 GHz for GPS application. The dual-band frequency is performed at 0.89 GHz and 2.45 GHz, UHF and ISM bands for RFID applications when the switches are ON state. The upper band of the antenna can be adjusted by varied the value of *d* and *b* of the C-shaped patch. The simulation of the radiation pattern gives an omnidirectional pattern for both single band and dual bands. The proposed antenna has been fabricated and tested and it showed good agreement between simulated and measured results.

REFERENCES

[1] H. Rajagopalan, J. M Kovitz, Y. Rahmat-Samii, "MEMS

reconfigurable optimized e-shaped patch antenna design for cognitive radio", *IEEE Trans. Antennas and Propagation*, vol. 62, no. 3, pp. 1056–1064, 2014. [Online]. Available: http://dx.doi.org/10.1109/TAP.2013.2292531

[2] Pei-Yuan Qin, Y. J Guo, Can Ding, "A dual-band polarization reconfigurable antenna for WLAN systems", *IEEE Trans. Antennas and Propagation*, vol. 61, no. 11, pp. 5706–5713, 2013. [Online]. Available: http://dx.doi.org/10.1109/TAP.2013.2279219

[3] H. F. Abu Tarboush, R. Nilavalan, S. W. Cheung, K. M. Nasr, T. Peter, D. Budimir, H. Raweshidy, "A reconfigurable wideband and multiband antenna using dual-patch elements for compact wireless devices", *IEEE Trans. on Antennas and Propagation*, vol. 60, no. 1, pp. 36–43, 2012. [Online]. Available: http://dx.doi.org/10.1109/TAP.2011.2167925

[4] L. Pazin, V. Leviatan, "Reconfigurable slot antenna for switchable multiband operation in a wide frequency range", *IEEE Antennas and Wireless Propagation Letters*, vol. 12, pp. 392–332, 2013. [Online]. Available: http://dx.doi.org/10.1109/LAWP.2013.2246855

[5] Chih-Hsiang Ko, I-young Tarn, Shyh-Jong Chung, "A compact dual-band pattern diversity antenna by dual-band reconfigurable frequency-selective reflectors with a minimum number of switches", *IEEE Trans. Antennas and Propagation*, vol. 61, no. 2, pp. 646–654, 2013. [Online]. Available: http://dx.doi.org/10.1109/TAP.2012.2225011

[6] I. H. Idris, M. R. Hamid, M. H. Jamaluddin, M. K. A. Rahim, H. A. Majid, "Multiband reconfigurable antenna for 2.4 GHz, 3.5 GHz & 5.2 GHz applications", *IEEE Wireless Technology and Application Symposium (ISWTA)*, 2013, pp. 245–248. [Online]. Available: http://dx.doi.org/10.1109/ISWTA.2013.6688780

[7] F. Paredes, G. Zamora, F. J. Herraiz-Martinez, F. Martin, J. Bonache, "Dual-band UHF-RFID tags based on meander-line antennas loaded with spiral resonators", I*EEE Antennas and Wireless Propagation Letters*, vol. 10, pp. 768–771, 2011. [Online]. Available: http://dx.doi.org/10.1109/LAWP.2011.2162716

[8] Jui-Han Lu, Chia-Luan Tang, Kin-Lu Wong, "Novel dual-frequency and broad-band designs of slot loaded equilateral triangular microstrip antennas", *IEEE Trans. Antennas and Propagation*, vol. 48, no. 7, pp. 1048–1054, 2000. [Online]. Available: http://dx.doi.org/10.1109/8.876323

[9] X. L. Bao, M. J. Amman, "Compact concentric annular-ring patch anntenna for triple-frequency operation", *Electronics Letters*, vol. 42, no. 20, pp. 1129–1130, 2006. [Online]. Available: http://dx.doi.org/10.1049/el:20062015

[10] R. L. Li, X. L. Quan, Y. H. Cui, M. M. Tentzeries, "Directional triple-band planar antenna for WLAN/WiMAX access points", *Electronics letters*, vol. 48, no. 62, pp. 305–306, 2012. [Online]. Available: http://dx.doi.org/10.1049/el.2011.3448

[11] Chen Yongqiang, Guo Huiping, Yang Xinmi, Liu Xueguan, "A low-profile dual-band RFID antenna combined with silence element", in *Proc. Int. Symposium on Antennas & Propagation*, vol. 2, pp. 1146–1149, 2013.

[12] S. Verma, P. Kumar, "Dual-band UHF-RFID tags based on meander-line antennas loaded with spiral resonators", *IEEE Antennas and Wireless Propagation Letters*, vol. 10, pp. 768–771, 2011. [Online]. Available: http://dx.doi.org/10.1109/LAWP.2011.2162716

[13] Kim Dongho, Yeo Jun Ho, "Dual-band long-range passive RFID tag antenna using an AMC ground plane", *IEEE Trans. Antennas and Propagation*, vol. 60, no. 6, pp. 2620–2626, 2012. [Online]. Available: http://dx.doi.org/10.1109/TAP.2012.2194638

[14] J. Y. Park, J. M Woo, "Miniaturised dual-band s-shaped RFID tag antenna mountable on metallic surface", *Electronics Letters*, vol. 44, no. 23, pp. 1339–1341, 2008. [Online]. Available: http://dx.doi.org/10.1049/el:20082102

[15] M. I. Sabran, S. K. A. Rahim, A. Y. A. Rahman, T. A. Rahman, M. Z. M. Nor, Evizal, "A dual-band diamond-shaped antenna for RFID application", *IEEE Trans. Antennas and Propagation*, vol. 10, pp. 979–982, 2011. [Online]. Available: http://dx.doi.org/10.1109/LAWP.2011.2168189

[16] Xu Zishu, Li Xiuping, "Aperture coupling two-layered dual-band RFID reader antenna design", *IEEE Int. Conf. Microwave and Millimeter Wave Technology*, vol. 3, pp. 1218–1221, 2008.

[17] Ma Zi Long, Li Jun Jiang, Xi Jingtian, T. T. Ye, "A single-layer compact HF-UHF dual-band RFID tag antenna", *IEEE Antennas and Wireless Propagation Letters*, vol. 11, pp. 1257–1260, 2012. [Online]. Available: http://dx.doi.org/10.1109/LAWP.2012.2225821

[18] Oh Kyoung-Sub, Son Wang-Ik, Cha Sung-Yong, Lee Moon Que, Yu Jong-Won, "Compact dual-bans printed quadrifilar antennas for UHF RFID/GPS operations", *IEEE Antennas and Wireless Propagation Letters*, vol. 10, pp. 804–807, 2011. [Online]. Available: http://dx.doi.org/10.1109/LAWP.2011.2163610

[19] W. L. Stutzmann, G. A. Thiele, *Antenna theory and design*. New York: John Wiley and Sons, 1998.

[20] Chen Yikai, Yang Shiwen, Nie Zaiping, "Bandwidth enhancement method for low profile e shaped microstrip patch antennas", *IEEE Trans. Antennas and Propagation*, vol. 58, no. 7, pp. 2442–2447, 2010. [Online]. Available: http://dx.doi.org/10.1109/TAP.2010.2048850

[21] Nanbo Jin, Y.Rahmat-Samii, "Design of e-shaped dual-band and wideband patch antenna using parallel PSO/FDTD algorithm", *IEEE Int. Symposium on Antennas and Propagation Society*, vol. 2A, 2005, pp. 37–40.

[22] A. Khidre, Lee Kai-Fong, Fan Yang, A. Z. Elsherbeni, "Circular polarization reconfigurable wideband e-shaped patch antenna for wireless applications", *IEEE Trans. Antennas and Propagation*, vol. 61, no. 2, pp. 960–964, 2013. [Online]. Available: http://dx.doi.org/10.1109/TAP.2012.2223436